

## ARTICLE OPEN

## Using the standard deviational ellipse to document changes to the spatial dispersion of seasonal tornado activity in the United States

Todd W. Moore<sup>1</sup> and Michael P. McGuire<sup>2</sup>

Recent studies have documented possible ongoing changes to the climatology of tornadoes in the United States. Observed changes include increasing tornado counts in the Southeast and Midwest Regions, decreasing tornado counts in the Great Plains, and increased clustering of tornadoes on fewer days of the year. This study illustrates that the spatial dispersion of tornadoes in the United States is also changing. The dispersion of tornadoes decreased between 1954 and 2017, most notably in spring, summer, and fall. Furthermore, tornadoes tended to be less spatially dispersed in seasons with more tornadoes and with multiple days on which 20 or more tornadoes occur. This suggests that the increased occurrence of tornado outbreaks is contributing to the decrease in dispersion.

*npj Climate and Atmospheric Science* (2019)2:21 ; <https://doi.org/10.1038/s41612-019-0078-4>

## INTRODUCTION

The body of literature focused on the potential link between climate change and tornado activity in the United States has grown over the past decade. One approach to this problem has been to use global climate models to examine future environmental conditions, such as instability and shear, that are favorable for tornadoes.<sup>1–10</sup> Such studies have generally concluded that future conditions will favor severe weather and tornadoes across portions of the eastern United States, largely because of increased surface temperature, low-level moisture, and instability. Another approach to the climate/tornado link is to document long-term trends in tornado activity. This study takes such an empirical approach by documenting changes in the spatial dispersion of tornadoes in the United States between 1954 and 2017.

Recent empirical studies illustrate that tornadoes are beginning to cluster more in time.<sup>11–17</sup> For example, the proportion of annual tornadoes occurring in outbreaks (six or more tornadoes with no longer than 6 h between successive start times) and the mean number of tornadoes per outbreak have increased over time.<sup>14</sup> The greatest rates of increase have been with the outbreaks with the most tornadoes.<sup>15</sup> The number of days per year with many tornadoes (e.g., 20+) and the proportion of tornadoes occurring on these days have also increased over time.<sup>11,13,16,17</sup> These changes have led to an increase in the mean and variability of the number of tornadoes per tornado outbreak and day.<sup>14,16</sup>

Recent empirical studies also illustrate that the spatial distribution of tornadoes has shifted over time by analyzing tornado density maps,<sup>17–19</sup> regional and gridded trends,<sup>17,20–22</sup> and trends in the center of tornado activity.<sup>17,23–25</sup> The observed maximum of gridded tornado and tornado day counts, for example, has shifted from the Great Plains to the Southeast between the periods 1954–1983 and 1984–2013.<sup>19</sup> Regional and gridded annual tornado counts have similarly trended downward in portions of

the Great Plains and upward throughout most of the Southeast.<sup>17,20–22</sup> The decrease in the Great Plains is observed in all seasons, whereas the increase in the Southeast is driven mostly by recent increases in tornado activity in winter and fall.<sup>17,22</sup> These regional trends have led to eastward shifts in the center of annual tornado activity and in spring, summer, and fall.<sup>17,25</sup> These observations of an eastward shift are consistent with projections of increased tornado-favorable environments in the Southeast.<sup>5,9</sup>

Changes in the temporal and spatial distributions of tornadoes have been documented,<sup>17–25</sup> but changes to the spatial dispersion, or the area over which most tornadoes are dispersed, have not been documented. This study, therefore, documents changes to the spatial dispersion of tornadoes in the United States. To do so, we calculate the standard deviational ellipse (SDE), a measure of spatial dispersion, of tornadoes rated 1 or higher by the Fujita or Enhanced Fujita ((E)F1+) damage rating scales between 1954 and 2017. Our results highlight seasonal changes in the spatial dispersion of tornadoes. They also illustrate that the area of the SDEs has changed over time, with notable decreases across the study period in summer and fall and in the last part of the record in winter and spring. Lastly, the results presented herein suggest that tornadoes tend to be more concentrated in seasons with more tornadoes and many days with a large number of tornadoes.

## RESULTS

## Standard deviational ellipsoid

The mean centers of the SDEs capture the seasonal shifts in tornado activity (Fig. 1a–d). In winter (December of previous year, January, February—DJF), tornado activity centers in the southeastern United States. The center of tornado activity migrates through the Great Plains and into the Midwest through spring (March, April, May—MAM) and summer (June, July, August—JJA).

<sup>1</sup>Department of Geography and Environmental Planning, Towson University, Towson, MD, USA and <sup>2</sup>Department of Computer and Information Sciences, Towson University, Towson, MD, USA

Correspondence: Todd W. Moore (tmoore@towson.edu)

Received: 28 December 2018 Accepted: 18 June 2019

Published online: 01 July 2019

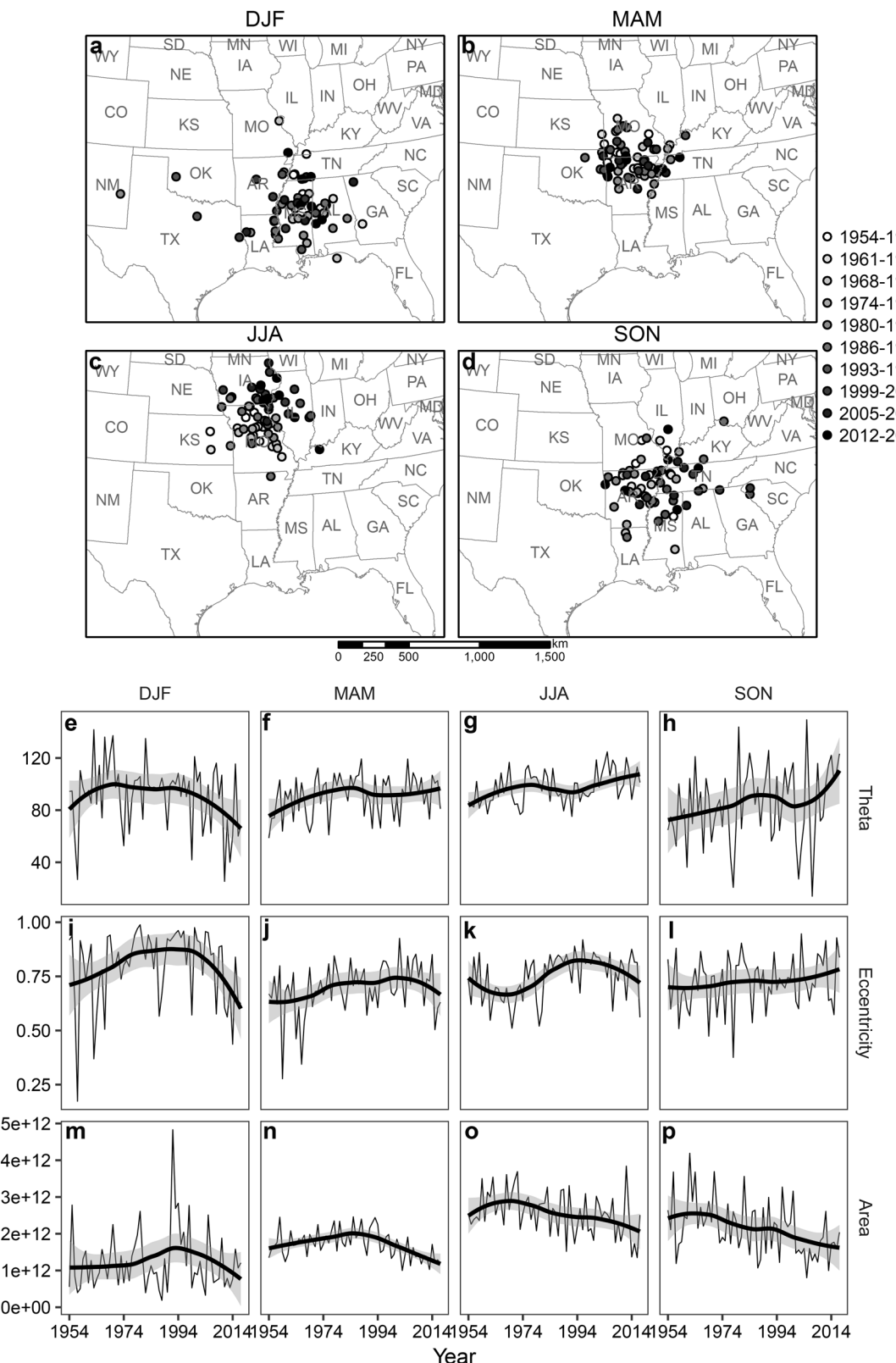


**Fig. 1** Mean centers (latitude ( $^{\circ}$ N), longitude ( $^{\circ}$ W)) of seasonal (E)F1+ tornadoes between 1954 and 2017, binned into 5-year intervals (a-d). Angle of rotation (theta ( $^{\circ}$ ), e-h), eccentricity (i-l), and area ( $m^2$ , m-p) of the SDEs for seasonal (E)F1+ tornadoes between 1954 and 2017. Local regression curves (with a neighborhood of 0.75) and 95% confidence intervals (CIs) are shown in e-p

**Table 1.** Mann-Kendall trend statistic ( $S$ ), Theil-Sen slope estimate ( $\beta$ ), and probability value ( $p$ )

	$S$	$\beta$	$p$
Mean center (°N and °W)			
Winter latitude	152	1.05E-02	3.82E-01
Winter longitude	-158	-1.42E-02	3.63E-01
Spring latitude	-174	-6.94E-03	3.16E-01
Spring longitude	248	1.54E-02	1.52E-01
Summer latitude <sup>a</sup>	850	4.17E-02	8.71E-07
Summer longitude <sup>a</sup>	522	3.30E-02	2.54E-03
Fall latitude	-84	-3.38E-03	6.31E-01
Fall longitude <sup>b</sup>	390	4.03E-02	2.42E-02
Theta (°)			
Winter	-180	-1.87E-01	3.00E-01
Spring	296	1.72E-01	8.74E-02
Summer <sup>a</sup>	562	2.52E-01	1.15E-03
Fall <sup>b</sup>	364	3.96E-01	3.55E-02
Eccentricity			
Winter	46	2.67E-04	7.94E-01
Spring <sup>b</sup>	358	1.45E-03	3.86E-02
Summer <sup>a</sup>	494	2.08E-03	4.29E-03
Fall	178	9.27E-04	3.05E-01
Area, 1954–2017 (m <sup>2</sup> )			
Winter	52	8.16E+08	7.68E-01
Spring <sup>b</sup>	-422	-6.34E+09	1.47E-02
Summer <sup>a</sup>	-473	-1.13E+10	6.24E-03
Fall <sup>a</sup>	-585	-1.63E+10	7.13E-04
Area, 1995–2017 (m <sup>2</sup> )			
Winter	-39	-2.23E+10	3.16E-01
Spring <sup>a</sup>	-93	-2.49E+10	1.51E-02
Summer	-39	-1.80E+10	3.16E-01
Fall	-41	-2.88E+10	2.91E-01
Area, 1954–2017 (m <sup>2</sup> )			
Sept–Mar <sup>b</sup>	-354	-6.96E+9	4.04E-02
Apr–Aug <sup>a</sup>	-496	-6.75E+9	4.13E-03

<sup>a</sup>Trends significant at  $\alpha = 0.01$ <sup>b</sup>Trends significant at  $\alpha = 0.05$ 

rotated clockwise) at a rate of 0.25° per year between 1954 and 2017 (Fig. 1g; Table 1). The eccentricity, which represents the ellipticity of the SDEs, also increased in JJA at a rate of 0.002 per year (Fig. 1k; Table 1). The angle of rotation also increased in MAM and SON, but trends are not significant at  $\alpha = 0.01$  (Fig. 1j, l; Table 1). In DJF, the angle of rotation was rather stable until the late 1990s at which time a decline (i.e., rotated counter-clockwise) is noticeable (Fig. 1e).

The area of the SDEs represents the concentration (or distribution density) of tornadoes.<sup>26,27</sup> The area varies across the seasons and is, in general, greater in JJA and SON than in DJF and MAM (Fig. 1m–p). The mean (median) area in DJF is 1.2E+12 m<sup>2</sup> (1.1E+12 m<sup>2</sup>); in MAM is 1.7E+12 m<sup>2</sup> (1.7E+12 m<sup>2</sup>); in JJA is 2.6E+12 m<sup>2</sup> (2.5E+12 m<sup>2</sup>); and in SON is 2.2E+12 m<sup>2</sup> (2.1E+12 m<sup>2</sup>). These differences in the area of the SDEs show that the dispersion of tornadoes changes across the seasons, with the greatest dispersion seen in JJA and SON and the greatest concentration seen in DJF and MAM. The area of the SDEs also significantly decreased in JJA and SON at rates of -1.13E+10 m<sup>2</sup> per year and -1.63E+10 m<sup>2</sup> per year, respectively (Fig. 1o, p; Table 1). The mean (median) area of the SDEs in JJA and SON were 2.81E+12 m<sup>2</sup> (2.79E+12 m<sup>2</sup>) and 2.50E+12 m<sup>2</sup> (2.41E+12 m<sup>2</sup>), respectively, in the earliest 25 years of the record (1954–1978). These values decreased by 4.89E+11 m<sup>2</sup> (4.70E+11 m<sup>2</sup>) and 6.59E+11 m<sup>2</sup> (6.80E+11 m<sup>2</sup>) to 2.32E+12 m<sup>2</sup> (2.32E+12 m<sup>2</sup>) and 1.84E+12 m<sup>2</sup> (1.73E+12 m<sup>2</sup>) in the last 25 years (1993–2017). The area covered by the SDEs in MAM also significantly declined (at a rate of -6.34E+09 m<sup>2</sup> per year), but the decline occurred only after the late-1980s (Fig. 1n). These decreases indicate that tornadoes have become less dispersed (more concentrated) over time.

The increased concentration of tornadoes is not a result of removing (E)F0 tornadoes from the record. Decreases in area are also observed for SDEs that include (E)F0+ tornadoes between 1995 and 2018 (Fig. 2). These trends, however, are not significant (Table 1), most likely due to the short period of record and the amount of inter-annual variability. The increased concentration of tornadoes also is not a result of our use of climatological seasons. Significant decreases in area are observed when considering tornadoes that occurred between September and March, when tornado activity is greatest in the Southeast and Midwest, and between April and August, when tornado activity is greatest in the Great Plains (Fig. 3; Table 1).

#### Association between SDE area and counts of tornadoes and days with many tornadoes

The number of tornadoes falling within the SDEs varies with the seasons, but there is no long-term trend (Fig. 4a–d). The percentage of tornadoes in a given year that fell within the SDEs is generally between 50 and 85% in all seasons, again with no long-term trends present (Fig. 4e–h). The absence of long-term trends in the counts and percentages of tornadoes within the SDEs show that the decrease in the area of the SDEs is not related to a decrease in the number of tornadoes falling within them. Although not all are statistically significant, there is actually a weak negative correlation between the area of the SDEs and the number of tornadoes falling within them (Fig. 5). The Spearman's  $\rho$  ( $\rho$ ) correlation coefficients and  $p$ -values ( $p$ ) are as follows: DJF  $\rho = -0.21$ ,  $p = 0.10$ ; MAM  $\rho = -0.27$ ,  $p = 0.03$ ; JJA  $\rho = -0.13$ ,  $p = 0.30$ ; and SON  $\rho = -0.44$ ,  $p < 0.01$ . This illustrates that SDEs with smaller areas tend to include a greater number of tornadoes. We also note that SDE area is also negatively related to the total number of (E)F1+ tornadoes (as opposed to the number occurring within the SDE), with correlation coefficients and  $p$ -values as follows: DJF  $\rho = -0.24$ ,  $p = 0.05$ ; MAM  $\rho = -0.27$ ,  $p = 0.03$ ; JJA  $\rho = -0.05$ ,  $p = 0.68$ ; and SON  $\rho = -0.38$ ,  $p < 0.01$ .

Moore and DeBoer<sup>17</sup> recently illustrated that the increasing frequency of days with many tornadoes (e.g., 20+ (E)F1+

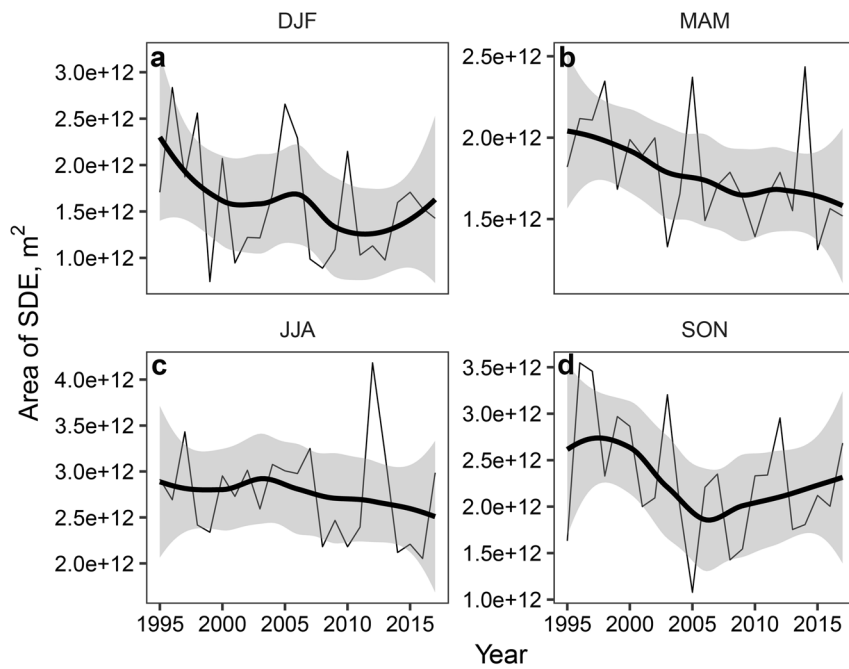


**Fig. 2** Area (m<sup>2</sup>) of SDEs for **a** winter (DJF), **b** spring (MAM), **c** summer (JJA), and **d** fall (SON) (E)F0+ tornadoes between 1995 and 2017. Local regression curves (with a neighborhood of 0.75) and 95% CIs are shown

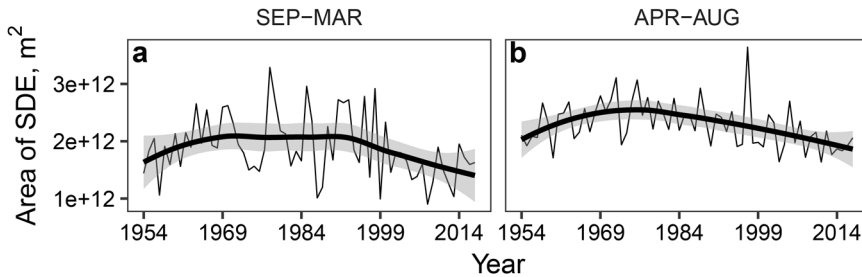


**Fig. 3** Area (m<sup>2</sup>) of SDEs for (E)F1+ tornadoes that occurred between September and March **a**, when tornado activity is greatest in the Southeast, and between April and August **b**, when tornado activity is greatest in the Great Plains. Local regression curves (with a neighborhood of 0.75) and 95% CIs are shown

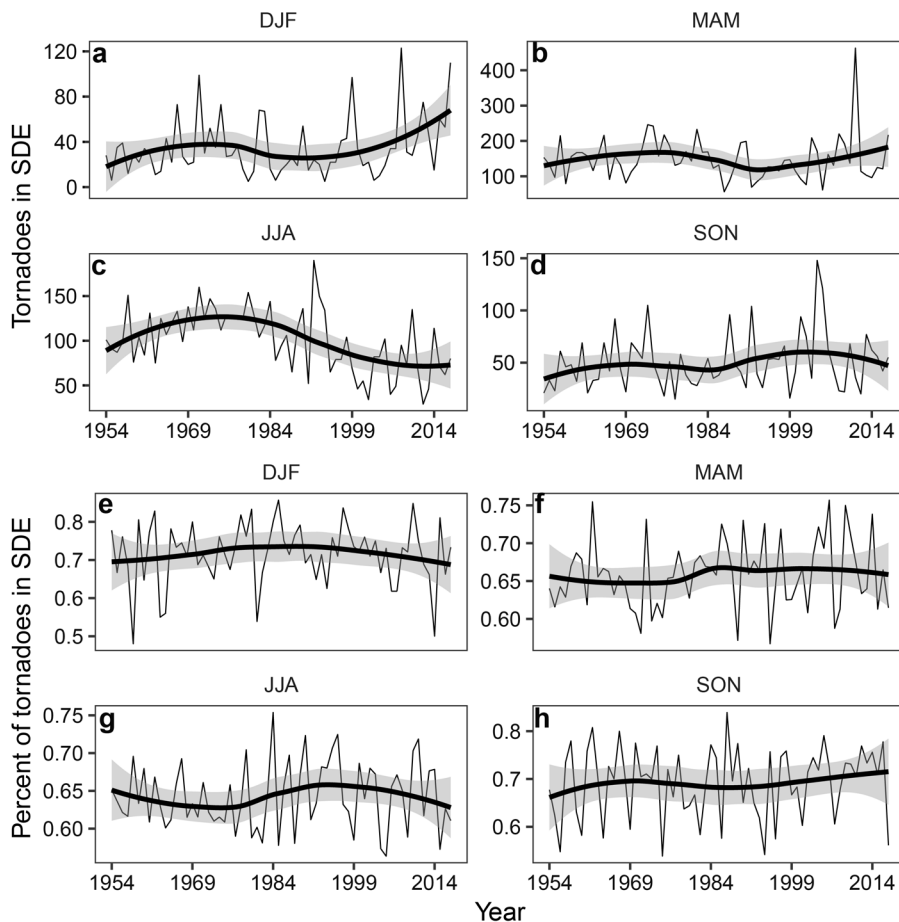
tornadoes) contributes to the eastward shift in tornado activity (i.e., the decreasing (increasing) trends in portions of the Great Plains (Southeast)) by showing that the tornadoes that occur on these days tend to concentrate in the Southeast. Because tornadoes that occur on these days tend to be relatively concentrated compared to climatology, and because the proportion of annual tornadoes occurring on these days is increasing,<sup>13</sup> it seems plausible that the increased frequency of these days may also be contributing to the decrease in dispersion.

Figure 6a-d illustrates that the area of the SDE tends to get smaller as the number of days (00 UTC–00 UTC) with 20+ (E)F1+ tornadoes increases, in all seasons. For example, the mean (median) areas in DJF, MAM, JJA, and SON in seasons when there are no days with 20+ tornadoes are 1.35E+12 m<sup>2</sup> (1.25E+12 m<sup>2</sup>), 1.91E+12 m<sup>2</sup> (1.94E+12 m<sup>2</sup>), 2.65E+12 m<sup>2</sup> (2.59E+12 m<sup>2</sup>), and 2.36E+12 m<sup>2</sup> (2.34E+12 m<sup>2</sup>), respectively. These decrease notably in seasons with more 20+ days. In DJF and MAM, for example, they decrease to 1.21E+12 m<sup>2</sup> (1.21E+12 m<sup>2</sup>) and 1.53E+12 m<sup>2</sup> (1.44E+12 m<sup>2</sup>) in seasons with only three 20+ days. They decrease to 1.85E+12 m<sup>2</sup> (1.77E+12 m<sup>2</sup>) and 1.54E+12 m<sup>2</sup> (1.56E+12 m<sup>2</sup>) in JJA and SON when two 20+ days occur. Furthermore, seasonal tornado counts tend to be greater in seasons with more 20+ (E)F1+ tornado days (Fig. 6e-h). This is further illustration that seasons

with the most concentrated tornado activity tend to have more (E)F1+ tornadoes and more days with a large number of tornadoes.

## DISCUSSION

The results of this study need to be considered in combination with those from other recent studies that provide empirical evidence of possible changes to the climatology of tornadoes in the United States.<sup>11–22</sup> The decreased area of the SDEs in SON, for example, accompanies an increase in the frequency of (E)F1+ tornadoes and days with 20+ (E)F1+ tornadoes, particularly in the Southeast.<sup>17</sup> Combined, these changes illustrate that tornado activity is increasing and becoming more concentrated toward the Southeast in SON. The decreased area of the SDEs in JJA, conversely, accompanies a decrease in the frequency of (E)F1+ tornadoes, particularly in the southern Great Plains.<sup>22</sup> The notable decrease in tornado activity in the southern Great Plains also contributes to the clockwise rotation over time of the SDEs in JJA. In the early period of record (e.g., 1954–1979), the SDEs in JJA extended over portions of the southern Great Plains. In the latter part of the record (e.g., 1990–2017), most SDEs were concentrated farther north and excluded the southern Great Plains (Supplementary Fig. 3 in supplemental material). Therefore, although the overall seasonal count of tornadoes may be decreasing in JJA, the



**Fig. 4** Seasonal (E)F1+ tornadoes falling within the SDEs between 1954 and 2017 shown as counts (a-d) and as percentages of (E)F1+ tornadoes occurring in the contiguous United States (e-h). Local regression curves (with a neighborhood of 0.75) and 95% CIs are shown

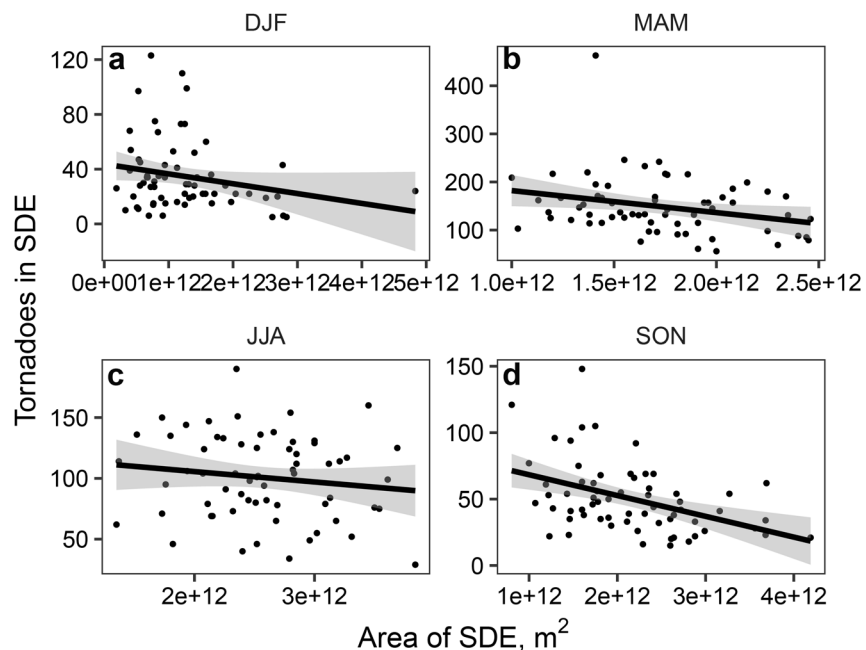


**Fig. 5** Relationship between the area of an SDE and the count of tornadoes falling within the SDE in **a** winter (DJF), **b** spring (MAM), **c** summer (JJA), and **d** fall (SON). Linear trend lines and 95% CIs are shown

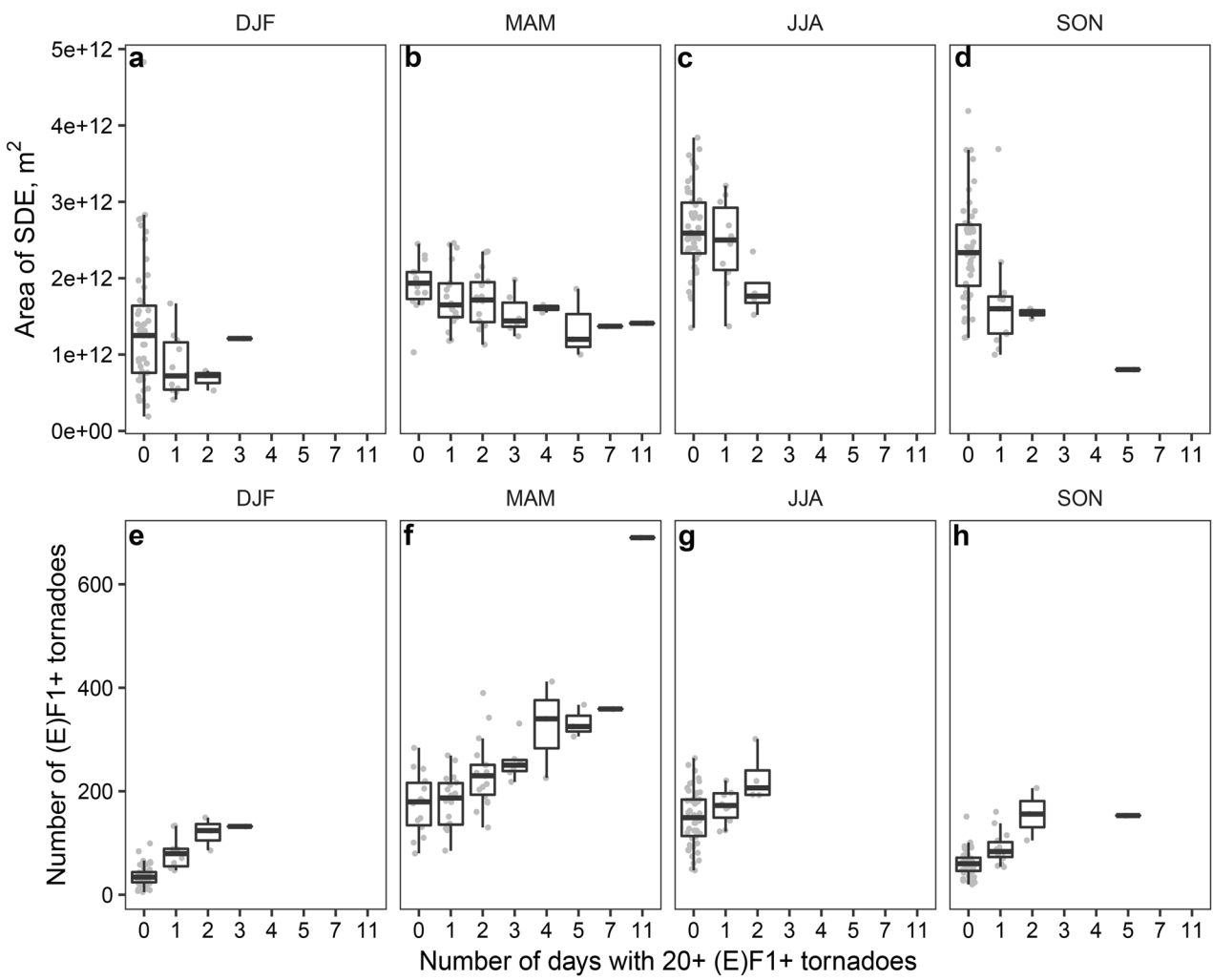


**Fig. 6** Distributions of SDE area ( $\text{m}^2$ ) for each of the observed number of days per year with 20+ (E)F1+ tornadoes (a–d). Distributions of the number of (E)F1+ tornadoes for each of the observed number of days per year with 20+ (E)F1+ tornadoes (e–h). Bottom of the boxes is set at the 25th percentile, top of the boxes at the 75th percentile, horizontal line within at the 50th percentile, and the whiskers extend to 1.5 times the inter-quartile range above and below the 75th and 25th percentiles

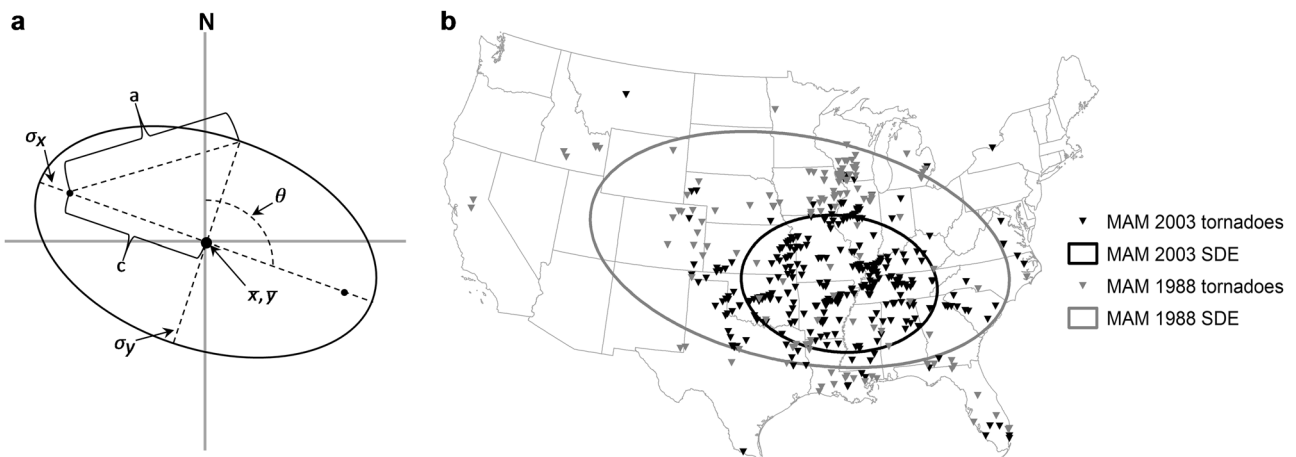


**Fig. 7** Conceptual illustration of an SDE **a** and examples of SDEs fit to the (E)F1+ tornadoes in MAM 2003 and 1988 **b**

risk is more concentrated and shifting slightly northeastward through the Great Plains and Midwest.

It was shown herein that (E)F1+ tornadoes tend to be less dispersed in seasons with more 20+ tornado days, and that the

decrease in dispersion over time is cooccurring with an increase in the frequency of these tornado-active days. Elsner et al.<sup>13</sup> similarly showed that the mean number of tornado clusters on days with 16+ (E)F1+ tornadoes trended upward between 1954 and 2013

and the total area of the clusters trended downward. They hypothesized that changes to local-scale thermodynamics (rather than larger-scale dynamics) is leading to fewer tornado days and to smaller but more active areas of severe convection on days with many tornadoes. Other research, however, illustrates that changes in wind shear are concordant with changes in tornado activity. Lu et al.<sup>28</sup>, for example, show that storm relative helicity, a metric of wind shear, plays an important role in the enhancement of peak tornado activity, and Tippett et al.<sup>15</sup> show that storm relative helicity, rather than instability, has increased over time conditional on the occurrence of extreme environments and tornado outbreaks. Gensini and Brooks<sup>22</sup> recently show that changes in the annual accumulation of the significant tornado parameter, which combines shear with other storm-relative wind and instability metrics, match changes in annual tornado counts, both of which have decreased throughout the Great Plains and increased throughout the Midwest and Southeast.

Additional research is needed to determine if other severe weather indices and climate variables correlate with the observed spatio-temporal changes in tornado activity. It is conceivable that changes to environmental conditions have essentially constricted the area over which tornadoes are most likely. Additional research is also needed to better understand the increasing frequency of tornado outbreaks<sup>11–17</sup> and potential links between their increased frequency and changes to the spatial dispersion (herein) and distribution<sup>17–25</sup> of tornadoes. The proportion of annual tornadoes that occur on days with many tornadoes is increasing,<sup>13</sup> and days with many tornadoes tend to occur in association with particular synoptic scale patterns and midlatitude cyclones.<sup>29–32</sup> It seems worthwhile to determine if the proportion of annual tornadoes being produced by these patterns is on the rise. It also seems worthwhile to search for changes in the midlatitude cyclone environment, such as more concentrated instability and/or shear, and for changes to the ambient environment into which cyclones that produce outbreaks move.<sup>33</sup>

A decrease in spatial dispersion suggests that the risk of tornadoes is focused over a smaller geographic area. Combining this with the increasing proportion of tornadoes occurring in the Southeast and Midwest further suggests that the risk is becoming more focused in these regions. Whether these changes are part of long-term variability or a sustained trend is yet to be seen. The increases observed in these regions, however, are consistent with projections that highlight them as areas favored for severe weather.<sup>5,9</sup> These trends do not eliminate the risk of tornadoes in other regions. Tornadoes have occurred in all 50 states and territories of the United States, and will do so in the future when suitable conditions are present. These trends also do not imply that tornado-related losses will increase in these regions. The ultimate impact that such trends will have on society also depends on the dynamic populations, built environments, and infrastructures that are exposed.<sup>20,34–37</sup>

## METHODS

### Tornado data

We use tornado data from the Storm Prediction Center's Severe Weather Database files (<https://www.spc.noaa.gov/wcm/>). The database currently covers the 1950–2017 period, but we subset to the 1954–2017 period to remove the notable undercount of tornadoes in the first few years.<sup>38</sup> December 1953 (2017) is included (excluded) because we analyzed seasonal tornado distributions. We also excluded tornadoes in Alaska, Hawaii, and Puerto Rico. Tornadoes rated 0 (lowest damage indicator) through 5 (highest damage indicator) by the Fujita (prior to February 2007) and Enhanced Fujita (beginning in February 2007) damage rating scales are included in the database. A notable increasing trend that is related mostly to technological advancements and increased detection and reporting of the weakest (E)F0 tornadoes over time, particular after the mid-1990s and the modernization of the Doppler radar network, is observed in the (E)F0+ record over the full 1954–2017 period.<sup>39</sup> Low

frequency variability is present in the (E)F1+ record, but the long term increasing trend is not.<sup>17</sup> We use both, the (E)F0+ and (E)F1+, records. The (E)F0+ record is used over the period 1995–2017 and the (E)F1+ record is used over the full 1954–2017 record.

### Standard deviational ellipse

We use the SDE as a measure of the dispersion of tornadoes. The SDE is designed to represent the geographic dispersion, or concentration, of objects.<sup>26,27</sup> SDEs tend to capture ~68% of objects that are normally distributed (spatially) about the mean center, but can capture fewer or more if the objects are overly dispersed or clustered.<sup>26,27</sup> Most SDEs in this study capture 50–85% of the tornadoes within a given season (Fig. 4e–h).

The SDE requires the calculation of the mean center of a distribution of points, the angle of rotation of the ellipse, and the SD along the x and y coordinates.<sup>40</sup> The SDE is centered on the mean center ( $\bar{x}, \bar{y}$ ), which is given by

$$\bar{x} = \frac{\sum x}{n}, \bar{y} = \frac{\sum y}{n} \quad (1)$$

where  $x$  and  $y$  are the start longitude and latitude, respectively, of the tornadoes (Fig. 7a).

The angle of rotation ( $\theta$ ) of the ellipse is given by

$$\tan \theta = \frac{(\sum x'^2 - \sum y'^2) + \sqrt{(\sum x'^2 - \sum y'^2)^2 + 4(\sum x'y')^2}}{2\sum x'y'} \quad (2)$$

where  $x'$  and  $y'$  are the deviations of the  $x$  and  $y$  coordinates from  $\bar{x}, \bar{y}$  (Fig. 7a).

The SDs along the  $x$  ( $\sigma_x$ ) and  $y$  ( $\sigma_y$ ) coordinates of the ellipse are given by (Fig. 7a)

$$\sigma_x = \sqrt{\frac{\sum (x' \cos \theta - y' \sin \theta)^2}{n}}, \sigma_y = \sqrt{\frac{\sum (x' \sin \theta - y' \cos \theta)^2}{n}} \quad (3)$$

The eccentricity ( $E$ ) of the ellipses is given by

$$E = \frac{c}{a} \quad (4)$$

where  $c$  is the distance between  $\bar{x}, \bar{y}$  and a focus and  $a$  is the distance from the focus to a vertex (Fig. 7a).

The area of the SDE ( $A$ ) is given by (Fig. 7a)

$$A = \pi \sigma_x \sigma_y \quad (5)$$

We calculated these ellipsoid characteristics for each season (winter (DJF), spring (MAM), summer (JJA), and fall (SON)) between 1954 and 2017 (using the (E)F1+ tornado record). We also calculated ellipsoid characteristics for each of these seasons between 1995 and 2017 (using the (E)F0+ tornado record) to assess the sensitivity of the analysis to the exclusion of (E)F0 tornadoes and for the periods September–March and April–August to assess the sensitivity of the analysis to our use of climatological seasons. Examples of SDEs for MAM 1988 and 2003 are provided in Fig. 7b. The SDEs for each season between 1954 and 2017 inclusive are shown in Supplementary Figs. 1–4.

### Trend test and slope estimation

When describing the rate of change over time of ellipsoid characteristics, we used the Mann–Kendall trend test<sup>41,42</sup> and Theil–Sen slope estimator.<sup>43,44</sup> The Mann–Kendall test statistic ( $S$ ) is given by

$$S = \sum_{i=1}^{n-1} \sum_{j=i+1}^n \text{sgn}(X_a - X_b) \quad (6)$$

where the sign of  $S$  corresponds to the direction of the trend,  $X_a$  and  $X_b$  are the sequential values in years  $a$  and  $b$ ,  $n$  is the number of years in the series, and

$$\text{sgn}(X_a - X_b) = \begin{cases} +1 & \text{for } X_a > X_b \\ 0 & \text{for } X_a = X_b \\ -1 & \text{for } X_a < X_b \end{cases} \quad (7)$$

The Theil–Sen slope ( $\beta$ ) is estimated with

$$\beta = \text{Median} \left[ \frac{X_a - X_b}{a - b} \right] \text{ for all } a < b \quad (8)$$

## DATA AVAILABILITY

Tornado data are freely available at <https://www.spc.noaa.gov/wcm/>. We used the 1950–2017\_actual\_tornadoes.csv file. SDE analyses were performed with the *aspase* package in R. Trend analyses were performed with the *trend* package in R. SDE data computed for this study are available from the corresponding author.

## AUTHOR CONTRIBUTIONS

T.W.M. conceived the study. M.P.M. performed the SDE analyses. T.W.M. performed the trend analyses, other statistical procedures, and prepared the figures. T.W.M. wrote the manuscript.

## ADDITIONAL INFORMATION

**Supplementary information** accompanies the paper on the *npj Climate and Atmospheric Science* website (<https://doi.org/10.1038/s41612-019-0078-4>).

**Competing interests:** The authors declare no competing interests.

**Publisher's note:** Springer Nature remains neutral with regard to jurisdictional claims in published maps and institutional affiliations.

## REFERENCES

1. Del Genio, A. D., Yao, M. S. & Jonas, J. Will moist convection be stronger in a warmer climate? *Geophys. Res. Lett.* **34**, L16703 (2007).
2. Trapp, R. J., Diffenbaugh, N. S., Brooks, H. E., Baldwin, M. E., Robinson, E. D. & Pal, J. S. Changes in severe thunderstorm environment frequency during the 21st century caused by anthropogenically enhanced global radiative forcing. *Proc. Natl Acad. Sci. USA* **104**, 19719–19723 (2007).
3. Trapp, R. J., Diffenbaugh, N. S. & Gluhovsky, A. Transient response of severe thunderstorm forcing to elevated greenhouse gas concentration. *Geophys. Res. Lett.* **36**, L01703 (2009).
4. Van Kooloer, S. L. & Roeber, P. J. Surface-based convective potential in the contiguous United States in a business-as-usual future climate. *J. Clim.* **22**, 3317–3330 (2009).
5. Lee, C. C. Utilizing synoptic climatology methods to assess the impacts of climate change on future tornado-favorable environments. *Nat. Hazard.* **62**, 325–343 (2012).
6. Brooks, H. E. Severe thunderstorms and climate change. *Atm. Res.* **123**, 129–138 (2013).
7. Diffenbaugh, N. S., Scherer, M. & Trapp, R. J. Robust increases in severe thunderstorm environments in response to greenhouse gas forcing. *Proc. Natl Acad. Sci. USA* **110**, 16361–16366 (2013).
8. Gensini, V. A. & Mote, T. L. Estimations of hazardous convective weather in the U. S. using dynamical downscaling. *J. Clim.* **27**, 6581–6598 (2014).
9. Gensini, V. A. & Mote, T. L. Downscaled estimates of late 21st century severe weather from CCSM3. *Clim. Change* **129**, 307–321 (2015).
10. Tippett, M. K., Allen, J. T., Gensini, V. A. & Brooks, H. E. Climate and hazardous convective weather. *Curr. Clim. Change. Rep.* **1**, 60–73 (2015).
11. Brooks, H. E., Carbin, G. W. & Marsh, P. T. Increased variability of tornado occurrence in the United States. *Science* **346**, 349–352 (2014).
12. Fuhrmann, C. M., Konrad, C. E. II, Kovach, M. M., McLeod, J. T., Schmitz, W. G. & Dixon, P. G. Ranking of tornado outbreaks across the United States and their climatological characteristics. *Weather Forecast* **29**, 684–701 (2014).
13. Elsner, J. B., Elsner, S. C. & Jagger, T. H. The increasing efficiency of tornado days in the United States. *Clim. Dyn.* **45**, 651–659 (2015).
14. Tippett, M. K. & Cohen, J. E. Tornado outbreak variability follows Taylor's power law of fluctuation scaling and increases dramatically with severity. *Nat. Commun.* **7**, 10668 (2016).
15. Tippett, M. K., Lepore, C. & Cohen, J. E. More tornadoes in the most extreme U.S. tornado outbreaks. *Science* **354**, 1419–1423 (2016).
16. Moore, T. W. On the temporal and spatial characteristics of tornado days in the United States. *Atm. Res.* **184**, 56–65 (2017).
17. Moore, T. W. & DeBoer, T. A. A review and analysis of possible changes to the climatology of tornadoes in the United States. *Prog. Phys. Geogr.* **43**, 365–390 (2019).
18. Farney, T. J. & Dixon, P. G. Variability of tornado climatology across the continental United States. *Int. J. Climatol.* **35**, 2993–3006 (2014).
19. Agee, E., Larson, J., Childs, S. & Marmo, A. Spatial redistribution of USA tornado activity between 1954 and 2013. *J. Appl. Meteorol. Climatol.* **55**, 1681–1697 (2016).
20. Ashley, W. S. & Strader, S. M. Recipe for disaster: how the dynamic ingredients of risk and exposure are changing the tornado disaster landscape. *Bull. Am. Meteorol. Soc.* **97**, 767–786 (2016).
21. Gensini, V. A. & Brooks, H. E. Spatial trends in United States tornado frequency. *npj Clim. Atm. Sci.* **1**, 38 (2018).
22. Moore, T. W. Annual and seasonal tornado trends in the contiguous United States and its regions. *Int. J. Climatol.* **38**, 1582–1594 (2018).
23. Fujita, T. T., Pearson, A. & Ludlum, D. M. Long-term fluctuation of tornado activities. In: 9th Conference Severe Local Storms, Norman, OK, American Meteorological Society (1975).
24. Schaefer, J. T., Kelly, D. L. & Abbey, R. F. A minimum assumption tornado-hazard probability model. *J. Clim. Appl. Meteorol.* **25**, 1934–1945 (1986).
25. Boruff, B. J., Easoz, J. A., Jones, S. D., Landry, H. R., Mitchem, J. D. & Cutter, S. L. Tornado hazards in the United States. *Clim. Res.* **24**, 103–117 (2003).
26. Yuill, R. S. The standard deviational ellipse; an updated tool for spatial description. *Geogr. Ann. Ser. B Hum. Geogr.* **53**, 28–39 (1971).
27. Gong, J. Clarifying the standard deviational ellipse. *Geogr. Anal.* **34**, 155–167 (2002).
28. Lu, M., Tippett, M. & Upmanu, L. Changes in the seasonality of tornado and favorable genesis conditions in the central United States. *Geophys. Res. Lett.* **42**, 4224–4231 (2015).
29. Doswell III, C. A., Weiss, S. J. & Johns, R. H. Tornado forecasting: a review. In: Church C, Burgess D, Doswell III CA, and Davies-Jones R (eds) *The Tornado: Its Structure, Dynamics, Prediction, and Hazards*. Washington DC: American Geophysical Union, 557–571 (1993).
30. Doswell, C. A. III, Carbin, G. W. & Brooks, H. E. The tornadoes of spring 2011 in the USA: an historical perspective. *Weather* **67**, 88–94 (2012).
31. Mercer, A. E., Shafer, C. M., Doswell, C. A. III, Leslie, L. M. & Richman, M. B. Synoptic composites of tornadic and nontornadic outbreaks. *Mon. Weather Rev.* **140**, 2590–2608 (2012).
32. Schultz, D. M., Richardson, Y. P., Markowski, P. M. & Doswell, C. A. III. Tornadoes in the central United States and the "clash of air masses." *Bull. Am. Meteorol. Soc.* **94**, 1704–1712 (2014).
33. Tochimoto, E. & Niino, H. Structural and environmental characteristics of extratropical cyclones that cause tornado outbreaks in the warm sector: a composite study. *Mon. Weather Rev.* **144**, 945–969 (2016).
34. Fricker, T., Elsner, J. B. & Jagger, T. H. Population and energy elasticity of tornado casualties. *Geophys. Res. Lett.* **44**, 3941–3949 (2017).
35. Strader, S. M., Ashley, W. S., Pingel, T. J. & Krmenev, A. J. Observed and projected changes in United States tornado exposure. *Weather Clim. Soc.* **9**, 109–123 (2017).
36. Strader, S. M., Ashley, W. S., Pingel, T. J. & Krmenev, A. J. Projected 21st century changes in tornado exposure, risk, and disaster potential. *Clim. Change* **141**, 301–313 (2017).
37. Elsner, J. B., Fricker, T. & Berry, W. D. A model for U.S. tornado casualties involving interaction between damage path estimates of population density and energy dissipation. *J. Appl. Meteorol. Climatol.* <https://doi.org/10.1175/JAMC-D-18-0106.1> (2018).
38. Agee, E. & Childs, S. Adjustments in tornado counts, F-scale intensity, and path width for assessing significant tornado destruction. *J. Appl. Meteorol. Climatol.* **53**, 1494–1505 (2014).
39. Verbout, S. M., Brooks, H. E., Leslie, L. M. & Schultz, D. M. Evolution of the US tornado database: 1954–2003. *Weather Forecast* **21**, 86–93 (2006).
40. Ebdon, D. *Statistics in Geography*. 2nd edn (Blackwell Publishers Ltd, Malden, MA, 1985).
41. Mann, H. B. Nonparametric tests against trend. *Econometrica* **13**, 245–259 (1945).
42. Kendall, M. G. *Rank Correlation Methods*. (Charles Griffin, London, 1975).
43. Theil, H. A rank-invariant method of linear and polynomial regression analysis. *Proc. K. Ned. Akad. van. Wet. Ser. A Math. Sci.* **53**, 386 (1950), 521, 1397–392 (part I), 525 (part II), 1412 (part III).
44. Sen, P. K. Estimates of the regression coefficient based on Kendall's tau. *J. Am. Stat. Assoc.* **63**, 1379–1389 (1968).



**Open Access** This article is licensed under a Creative Commons Attribution 4.0 International License, which permits use, sharing, adaptation, distribution and reproduction in any medium or format, as long as you give appropriate credit to the original author(s) and the source, provide a link to the Creative Commons license, and indicate if changes were made. The images or other third party material in this article are included in the article's Creative Commons license, unless indicated otherwise in a credit line to the material. If material is not included in the article's Creative Commons license and your intended use is not permitted by statutory regulation or exceeds the permitted use, you will need to obtain permission directly from the copyright holder. To view a copy of this license, visit <http://creativecommons.org/licenses/by/4.0/>.

© The Author(s) 2019